Stabilizing and Maneuvering Angle Rigid Multiagent Formations With Double-Integrator Agent Dynamics

Liangming Chen, *Member, IEEE*, Mingming Shi, Hector Garcia de Marina, and Ming Cao, *Fellow, IEEE*

***Abstract*—This article studies 2-D formation stabilization and maneuvering of mobile agents governed by double-integrator dynamics. The desired formation is described by a set of triple-agent interior angles. A carefully chosen such set of angle constraints guarantees that the desired formation is angle rigid. To achieve the desired angle rigid formation, a stabilization control law is proposed using only local velocity and direction measurements. We show that the closed-loop dynamics of the formation, when each agent is modeled by a double-integrator, are closely related to the corresponding one in single-integrator agent dynamics. Sufficient conditions are constructed to guarantee the closed-loop stability for identical and distinct velocity damping gains, respectively. To guide an angle rigid formation to move with the desired translational velocity, orientation, and scale, formation maneuvering laws are then proposed. Simulation examples are also provided to validate the results.**

***Index Terms*—Angle rigid formations, direction measurements, double-integrator agent dynamics, formation maneuvering, formation control, multiagent systems.**

I. Introduction

RECENTLY, multiagent formations have been widely studied due to their broad applications in, e.g., search and rescue using mobile robots [1], drone light shows [2], and formation flying of multiple satellites [3]. Two research problems arise, i.e., formation stabilization and formation maneuvering [4]. Under different specifications of formation shapes and available sensor measurements, different approaches have been proposed to solve these two problems [5].

Manuscript received 28 May 2021; revised 15 October 2021 and 30 December 2021; accepted 6 February 2022. Date of publication 25 February 2022; date of current version 19 September 2022. The work of Hector Garcia de Marina was supported by the Ramon y Cajal under Grant RYC2020-030090-I from the Spanish Ministry of Science. Recommended by Associate Editor Claudio Altafini. *(Corresponding author: Liangming Chen.)*

Liangming Chen and Ming Cao are with the Faculty of Science and Engineering, University of Groningen, 9747 Groningen, The Netherlands (e-mail: liangmingchen2018@gmail.com; ming.cao@ieee.org).

Mingming Shi is with the ICTEAM Institute, UCLouvain, 1348 Louvain-la-Neuve, Belgium (e-mail: mingming.shi@uclouvain.be).

Hector Garcia de Marina is with the Department of Computer Architecture and automation, University of Granada, 18011 Granada, Spain (e-mail: hgarciad@ieee.org).

Digital Object Identifier 10.1109/TCNS.2022.3153885

To achieve a formation specified by relative positions, a formation stabilization law is proposed in [6] by using the measurements of relative positions, in which the alignment of the coordinate frames of all the agents is required. In some scenarios, however, it can be difficult for all the agents to guarantee the perfect alignment of their coordinate frames due to the lack of a global reference and existence of sensor measurement noise. When misalignment exists in agents' coordinate frames, a distorted formation shape and nonzero translational velocity may appear in the relative position-specified formation [7], [8]. Without the requirement on coordinate frames' alignment, using distance rigidity theory, a desired formation described by distances is achieved using local relative position measurements in [9] and [10]. For the translation and rotation of distance rigid formations, several formation maneuvering algorithms are designed in [11]–[13] by employing a mismatch-based approach. Besides translational and rotational maneuvering, the scaling maneuvering is also necessary in many scenarios, e.g., obstacle avoidance [4], which, however, due to the pairwise distance change between agents during scaling, is not straightforward to be obtained by directly modifying the algorithms in [11]–[13]. Intuitively, bearing/angle constraints remain the same under scaling motion and, thus, can be utilized for both formation shape control and scaling maneuvering. Recently, it is reported that bearing/direction measurements can be obtained by monocular cameras, passive sonars and sensor arrays [14], [15], which are more accessible than relative position measurements. These developments promote the application of bearing rigidity theory and bearing-only formation control algorithms [16], which, however, require the alignment of coordinate frames of all the agents.

Not requiring the alignment of coordinate frames, a triangular formation control algorithm is proposed in [17] and [18] by employing triple-agent interior angles to specify the formation shape and using local inter-agent directions as the measurements. Further, [15] and [18], study angle rigidity and extend the results of [17] to formation stabilization with an arbitrary number of agents. According to [27], angle rigid formations enjoy more freedom than both distance and bearing rigid formations because the angle preservation motions allow simultaneous translation, rotation, and scaling. Given more degrees of freedom, angle rigid formations can be achieved using fewer

sensor measurements, and can choose more maneuvering forms to achieve practical tasks. By exploiting this advantage, maneuvering algorithms are proposed in [19] and [27] for angle rigid formations with single-integrator agent dynamics following a mismatch-based approach. However, to the authors' best knowledge, it has not been investigated how to stabilize and maneuver angle rigid formations with double-integrator agent dynamics, which is closer to real applications since double-integrator models capture better forces and moments in real mechanical systems [20, Ch. 2].

Motivated by the aforementioned works, this article aims at designing control algorithms for double-integrator multiagent systems by using local velocity and direction measurements to achieve the formation stabilization task, and by using the measurements of velocity, direction, and one relative position to achieve the desired translational, rotational, and scaling maneuvering. The contributions of this article can be summarized as follows.

1) The stabilization and maneuvering of angle rigid formations with double-integrator agent dynamics are realized. Although the structure of the double-integrator angle rigid formation's angle error dynamics is quite different from the corresponding one in single-integrator formations, we show that the closed-loop dynamics of the formation when the agents are governed by double-integrator dynamics are closely related to those of the corresponding single-integrator agent dynamics.

2) For the formation stabilization control law, only local velocity and direction measurements are needed. Compared to the stabilization of double-integrator formations using relative position measurements [21], [22], no distance measurements are required in our formation stabilization control law. For the formation maneuvering law, in addition to the measurements mentioned in the stabilization case, we require only one agent, to measure its relative position with respect to a reference agent. This relative position will be used to control the rotational and scaling maneuvering of the formation.

3) The desired maneuvering in forms of translation, rotation, and scaling is achieved simultaneously. Compared to the formation specified by relative positions, distances or bearings, angle rigid formations have more maneuvering degrees of freedom, which is helpful for those tasks requiring the formation to maneuver in translation, rotation, and scaling such that it passes through an unknown environment with obstacles.

The rest of this article is organized as follows. Section II introduces basic background knowledge and formulates the problem. In Section III, we present the results about the stabilization of angle rigid formations under identical and distinct control gains, respectively. The formation maneuvering algorithm and its stability analysis are given in Section IV. Simulation examples are provided in Section V. Finally, Section VI concludes this article.

II. Problem Formulation and Preliminaries

In this section, we introduce the agent dynamics, direction measurements, and angle rigid formations. Then, the research problem is formulated.

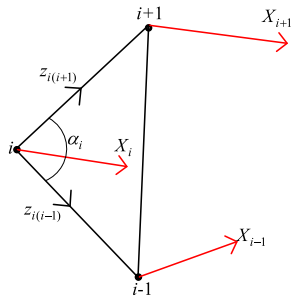

Fig. 1. Direction measurements.

A. Agents' Double-Integrator Dynamics

Consider N mobile agents moving in the plane. Agents are labeled from 1 to N, and $\mathcal{V} = \{1, 2, \ldots, N\}$ is the index set. The dynamics of each agent $i, i \in \mathcal{V}$, is governed by

$$\dot{p}_i = v_i, \dot{v}_i = u_i \tag{1}$$

where $p_i \in \mathbb{R}^2$ denotes the position of agent i with respect to a fixed global coordinate frame, $v_i \in \mathbb{R}^2$ is its velocity in the same frame, and $u_i \in \mathbb{R}^2$ is its control input to be determined.

B. Direction Measurements

Each agent $i \in \mathcal{V}$ can measure the "direction" with respect to some other agent $j \in \mathcal{V}$ with $p_i \neq p_j$, denoted by

$$z_{ij} := \frac{p_j - p_i}{\|p_j - p_i\|}$$

which is the unit vector starting from p_i and pointing towards p_j. The set of such j to which i measures its direction is denoted by $\mathcal{N}_i$, and for different i, $\mathcal{N}_i$ can be different. For the triangle formed by agents $i, i+1$ and $i-1$ shown in Fig. 1, the interior angle $\alpha_{(i+1)i(i-1)} \in [0, \pi]$ can be calculated by $\alpha_{(i+1)i(i-1)} = \arccos(z_{i(i+1)}^T z_{i(i-1)})$.

C. Construction of the Desired Angle Rigid Formation

To guarantee that the desired formation is unique under the given angle constraints, the formation is required to be *angle rigid* [18]. Now, we briefly introduce how to construct an angle rigid formation through a sequence of steps, which is similar to a sequence of Henneberg vertex addition steps [23]. For more details about angle rigidity, we refer the readers to [18]. First, we define an angle set $\mathcal{A} \subset \mathcal{V} \times \mathcal{V} \times \mathcal{V}$ to describe the angle constraints, where each member of $\mathcal{A}$ has three ordered vertices. The desired formation is recursively constructed by completing the following algorithm consisting of $N-2$ steps:

Step 1: The first three entries of $\mathcal{A}$ correspond to the three interior angles of the triangle $\triangle 123$, i.e., $\alpha_{312}, \alpha_{123}, \alpha_{231}$. Then, the eventual orientation and scale of the whole formation are determined by the orientation and scale of the first triangular formation, respectively.

Step 2: Add vertex 4 to the formation. This requires the knowledge of the next two elements of $\mathcal{A}$, which must be one of the following three combinations: 142 and 243, 142 and 143, or

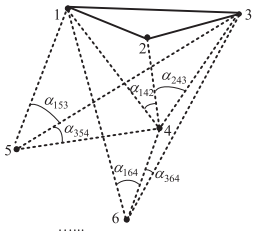

Fig. 2. Construction of an angle rigid formation.

243 and 143. In this article, we consider the combination α_{142} and α_{243} which is shown in Fig. 2.

Steps $3 \sim (N-3)$: Similar to Step 2, at each step, add a new vertex with two associated new angle constraints.

Step $(N-2)$ (last step): Add vertex N by adding two angle constraints: $\alpha_{i_1Ni_2}$ and $\alpha_{i_2Ni_3}$, $i_1, i_2, i_3 \in \{1, \ldots, N-1\}, i_1 \neq i_2 \neq i_3$.

As described in the above $N-2$ steps, the angle set is $\mathcal{A} = \{(3,1,2),(1,2,3),(2,3,1),(1,4,2),(2,4,3),\cdots,(j_1,k,j_2),(j_2,k,j_3),\ldots,(i_1,N,i_2),(i_2,N,i_3)\}$. Then, for $(j,i,k) \in \mathcal{A}$, we define $\{j,k\} \in \mathcal{N}_i$. According to the Type-I vertex addition operation in [18] and [18, Prop. 2], one has that the above constructed formation is generically angle rigid. To guarantee the uniqueness of each new vertex's position in Step i, $i = 2, \ldots, N-2$, the following assumption is needed.

Assumption 1: In each aforementioned Step $k-2, k = 4, \ldots, N$ with the corresponding angle constraints $\alpha_{j_1ij_2}$ and $\alpha_{j_2ij_3}$, we assume that $\alpha_{j_1ij_2}$ and $\alpha_{j_2ij_3}$ are not zero or π, $p_i, p_{j_1}, p_{j_2}, p_{j_3}$ are not on a circle, $\alpha_{j_1ij_3} = \alpha_{j_1ij_2} + \alpha_{j_2ij_3}$, $\sin\alpha_{j_1j_2i} > \sin\alpha_{ij_1j_2}$, and $\sin\alpha_{ij_2j_3} > \sin\alpha_{j_2j_3i}$.

Remark 1: According to [18, Prop. 2], when Assumption 1 holds, the position of each new vertex $k, k = 4, \ldots, N$ is locally uniquely determined,[1] which implies that the constructed formation is angle rigid. The inequalities in Assumption 1 are used to guarantee the single-integrator angle rigid formation locally stable[18, Th. 8]. Compared to [21] and [24], the construction of angle rigid formations is based on the Type-II vertex addition operation[18, Definition 7], under which the interagent communication is avoided in the control design and the number of angle constraints is minimized.

D. Problem Formulation

Consider that all the agents are governed by the double-integrator dynamics (1), and the desired formation is constructed by following the steps given in Section II-C. The goal is to design control input u_i for each agent i such that the whole multiagent system can achieve formation stabilization or formation maneuvering described formally as follows.

1) Formation stabilization: Each agent's position $p_i(t)$ converges to a fixed point which satisfies the angle constraints given in the desired angle rigid formation, and the velocities of all agents converge to zero, i.e.,

$$\lim_{t\to\infty} \dot{p}_i(t) = 0, \quad \forall i \in \mathcal{V}. \tag{2}$$

[1]This represents that the position of the added vertex is locally unique when all the vertices are perturbed within a small continuous neighborhood of the original configuration, but might not unique when the perturbation is large or in another nonneighboring region.

Note that when all the angle constraints are satisfied, one has that the first three agents achieve the desired triangular shape

$$\lim_{t\to\infty} e_i(t) = 0 \quad \forall i = 1,2,3 \tag{3}$$

where $e_i(t) = \alpha_i(t) - \alpha_i^*$, $\alpha_i = \alpha_{[i+1]i[i-1]}$, $[i+1] = 1$ when $i = 3$, $[i-1] = 3$ when $i = 1$, and $\alpha_i^* \in (0,\pi)$ denotes agent i's desired interior angle formed with agents $[i+1], [i-1]$, and naturally $\alpha_1^* + \alpha_2^* + \alpha_3^* = \pi$. Also note that each agent from 4 to N achieves the desired two angles

$$\lim_{t\to\infty} e_{i1}(t) = \lim_{t\to\infty}(\alpha_{j_1ij_2}(t) - \alpha^*_{j_1ij_2}) = 0 \tag{4}$$

$$\lim_{t\to\infty} e_{i2}(t) = \lim_{t\to\infty}(\alpha_{j_2ij_3}(t) - \alpha^*_{j_2ij_3}) = 0 \tag{5}$$

where $i = 4, \ldots, N$, $j_1 < i, j_2 < i, j_3 < i$, and $\alpha^*_{j_1ij_2} \in (0,\pi), \alpha^*_{j_2ij_3} \in (0,\pi)$ denote agent i's two desired angles formed with different agents $j_1, j_2, j_3 \in \{1,2,\ldots,i-1\}$. The available measurement information of each agent $i, i \in \mathcal{V}$ consists of velocity v_i and direction b_{ij} with respect to neighboring agents j in agent i's local coordinate frame.

2) Formation maneuvering: all the agents achieve the angle rigid formation described in (3)–(5), and the velocities of all the agents converge to a desired translational velocity $v_c^*(t) \in \mathbb{R}^2$, and the relative position from a reference agent (chosen to be agent 1) to another agent (for example, agent 3) will determine the eventual formation's orientation and scale. In particular, in this article, we will consider a piecewise constant vector $\delta_{13}^*(t) \in \mathbb{R}^2$ for the orientation and scale reference. The last two requirements in the formation maneuvering can be mathematically described by

$$\lim_{t\to\infty} (\dot{p}_i(t) - v_c^*(t)) = 0, \quad \forall i \in \mathcal{V} \tag{6}$$

$$\lim_{t\to\infty} (p_3(t) - p_1(t) - \delta_{13}^*(t)) = 0. \tag{7}$$

Therefore, the formation maneuvering task defined in this article requires all the agents to achieve (3)–(7) simultaneously. In this maneuvering case, each agent can measure its own velocity and the directions with respect to its neighbors, and agent 3 must measure its relative position with respect to agent 1.

III. Formation Stabilization

In this section, we discuss formation stabilization using identical and distinct control gains, respectively.

A. Case of Identical Control Gains

We first consider the situation when all the agents have the same velocity feedback gain. Specifically, we design the formation stabilization law as

$$u_i = -k_s v_i - \sum\nolimits_{(j,i,k)\in\mathcal{A}} (\alpha_{jik} - \alpha^*_{jik})(z_{ij} + z_{ik}) \tag{8}$$

where the gain $k_s > 0$ applies to all the agents. The control law (8) consists of a velocity damping part and an angle error feedback part, where the intuition of using $z_{ij} + z_{ik}$ is that it points toward the bisector of α_{jik}[18]. To obtain the convergence of angle errors under (8), we need to analyze their dynamics. First, we assume that $l_{ij}(0), l_{ik}(0)$ and $\sin\alpha_{jik}(0) \ \ \forall (j,i,k) \in \mathcal{A}$ are finite and bounded away from zero where $l_{ij}(t) = \|p_i(t) - p_j(t)\|$. According to (8), when the initial velocity $v_i(0)$ is bounded and $l_{ij}(0) \neq 0, l_{ik}(0) \neq 0$, the

control input $u_i(0)$ will be bounded. Therefore, $\exists T_1 > 0$ such that for $t \in [0, T_1)$, $l_{ij}(t), l_{ik}(t)$ and $\sin\alpha_{jik}(t) \quad \forall (j,i,k) \in \mathcal{A}$ are bounded away from zero. We now analyze the angle error dynamics for $t \in [0, T_1)$ and the extension of T_1 to infinity will be discussed later. Since $\frac{\mathrm{d}(\cos\alpha_{jik})}{\mathrm{d}t} = -(\sin\alpha_{jik})\dot{\alpha}_{jik}$, one has

$$\dot{\alpha}_{jik} = -\frac{1}{\sin\alpha_{jik}}\left(\frac{\mathrm{d}(\cos\alpha_{jik})}{\mathrm{d}t}\right). \tag{9}$$

Also, one has

$$\begin{aligned}\frac{\mathrm{d}(\cos\alpha_{jik})}{\mathrm{d}t} &= \frac{\mathrm{d}\left(z_{ij}^T z_{ik}\right)}{\mathrm{d}t} = \dot{z}_{ij}^T z_{ik} + z_{ij}^T \dot{z}_{ik} \\ &= z_{ik}^T \frac{P_{z_{ij}}}{l_{ij}}(v_j - v_i) + z_{ij}^T \frac{P_{z_{ik}}}{l_{ik}}(v_k - v_i) \end{aligned} \tag{10}$$

where $P_{z_{ij}} = I_2 - z_{ij} z_{ij}^T$, $I_2 \in \mathbb{R}^{2\times 2}$ is the 2×2 identity matrix. Substituting (10) into (9) yields

$$\begin{aligned}\dot{\alpha}_{jik} = & -z_{ik}^T \frac{P_{z_{ij}}}{l_{ij}\sin\alpha_{jik}} v_j - z_{ij}^T \frac{P_{z_{ik}}}{l_{ik}\sin\alpha_{jik}} v_k \\ & + \left(z_{ik}^T \frac{P_{z_{ij}}}{l_{ij}\sin\alpha_{jik}} + z_{ij}^T \frac{P_{z_{ik}}}{l_{ik}\sin\alpha_{jik}}\right) v_i. \end{aligned} \tag{11}$$

Let us choose the error variables defined in (2)–(5) to be the system state

$$X = [e_1, e_2, e_{41}, e_{42}, \ldots, e_{N1}, e_{N2}, v_1^T, \ldots, v_N^T]^T \in \mathbb{R}^{4N-4} \tag{12}$$

which consists of $2N-4$ independent angle errors and all agents' velocities. Then, from (8) and (11), one can check that the closed-loop dynamics satisfy

$$\dot{X} = \begin{bmatrix} 0_{(2N-4)\times(2N-4)} & R(X) \\ B(X) & -k_s \otimes I_{2N} \end{bmatrix} X = D_1(X) X \tag{13}$$

where $R(X) \in \mathbb{R}^{(2N-4)\times 2N}$ and $B(X) \in \mathbb{R}^{2N\times(2N-4)}$ are shown at the bottom of this page, and

$$N_{jik} = z_{ij}^T \frac{P_{z_{ik}}}{l_{ik}\sin\alpha_{jik}} \in \mathbb{R}^{1\times 2}, j, i, k \in \mathcal{V}$$

Now, we linearize (13) around the desired equilibrium $X = 0$ to study its local stability. By linearizing (13) around $X = 0$ for $t \in [0, T_1)$, one has

$$\begin{aligned}\dot{X} &= \left[\frac{\partial [D_1(X)X]}{\partial X}|_{X=0}\right] X = [D_1(X)|_{X=0}]X \\ &= \begin{bmatrix} 0_{(2N-4)\times(2N-4)} & R(X)|_{X=0} \\ B(X)|_{X=0} & -k_s \otimes I_{2N} \end{bmatrix} X = D_1^* X. \end{aligned} \tag{16}$$

For notation conciseness in the following analysis, a quantity with the superscript $*$ means that it is evaluated at $X = 0$. Note that the structure of the system matrix D_1^* in this double-integrator formation is quite different from the corresponding system matrix in the single-integrator formation[18, Eqs. (32) and (46)], which makes the formulated problem challenging. We then show that system (16) is stable by checking that $D_1^* \in \mathbb{R}^{4N-4}$ is Hurwitz through examining its eigenvalues. Consider the characteristic polynomial of D_1^*

$$|\lambda I_{4N-4} - D_1^*| = \begin{vmatrix} \lambda I_{2N-4} & -R^* \\ -B^* & (\lambda + k_s) \otimes I_{2N} \end{vmatrix} \tag{17}$$

where $\lambda \in \mathbb{C}$ is an eigenvalue of D_1^*. According to the Schur complement theorem [25], one has

$$\begin{aligned} & |\lambda I_{4N-4} - D_1^*| \\ &= (\lambda + k_s)^{2N} \det\left[\lambda I_{2N-4} - \frac{R^* B^*}{\lambda + k_s}\right] \\ &= (\lambda + k_s)^{2N} \det\left[\frac{\lambda(\lambda + k_s) I_{2N-4} - R^* B^*}{\lambda + k_s}\right] \\ &= (\lambda + k_s)^4 \det[\lambda(\lambda + k_s) I_{2N-4} - R^* B^*]. \end{aligned} \tag{18}$$

Hence, $-k_s$ is a stable eigenvalue of geometric multiplicity at least 4. To find the other eigenvalues, we now analyze the structure of the matrix $R^* B^*$. For the first three-agent case, one has the corresponding submatrix

$$[RB]_{(1:2,1:2)} = \tilde{F}_1 = \begin{bmatrix} a_{11} & a_{12} \\ a_{21} & a_{22} \end{bmatrix} \tag{19}$$

where $[RB]_{(i:j,k:m)}$ is the submatrix selecting rows from i to j and columns from k to m from the matrix RB. Therefore, it

$$R(X) = \begin{bmatrix} N_{213} + N_{312} & -N_{312} & -N_{213} & 0 & \ldots & 0 \\ -N_{321} & N_{321} + N_{123} & -N_{123} & 0 & \ldots & 0 \\ -N_{241} & -N_{142} & 0 & N_{142} + N_{241} & \ldots & 0 \\ \ldots & \ldots & \ldots & \ldots & \ldots & \ldots \end{bmatrix} \tag{14}$$

$$B(X) = \begin{bmatrix} -z_{12} - z_{13} & 0 & 0 & 0 & \ldots & 0 \\ 0 & -z_{21} - z_{23} & 0 & 0 & \ldots & 0 \\ z_{31} + z_{32} & z_{31} + z_{32} & 0 & 0 & \ldots & 0 \\ 0 & 0 & -z_{41} - z_{42} & -z_{42} - z_{43} & \ldots & 0 \\ \ldots & \ldots & \ldots & \ldots & \ldots & \ldots \end{bmatrix} \tag{15}$$

follows that:

$$a_{11} = (N_{213} + N_{312})(-z_{12} - z_{13}) - N_{213}(z_{31} + z_{32})$$
$$a_{12} = N_{312}(z_{21} + z_{23}) - N_{213}(z_{31} + z_{32})$$
$$a_{21} = N_{321}(z_{12} + z_{13}) - N_{123}(z_{31} + z_{32})$$
$$a_{22} = (N_{321} + N_{123})(-z_{21} - z_{23}) - N_{123}(z_{31} + z_{32}).$$

Since $P_{z_{ij}} z_{ij} = 0$ and $N_{312} z_{12} = 0$, one obtains $\tilde{F}_1 = \begin{bmatrix} N_{213}(z_{21} + z_{23}) - N_{312} z_{13} & (N_{312} + N_{213}) z_{23} \\ (N_{321} + N_{123}) z_{13} & N_{123}(z_{13} + z_{12}) - N_{321} z_{23} \end{bmatrix}$.

Substituting the definition of N_{jik} given after (14) into a_{11} yields

$$\begin{aligned} a_{11} &= \frac{z_{12}^T P_{z_{13}}(z_{21} + z_{23})}{l_{13} \sin\alpha_1} - \frac{z_{13}^T P_{z_{12}} z_{13}}{l_{12} \sin\alpha_1} \\ &= \frac{p_{12}^T P_{z_{13}}}{l_{12} l_{13} \sin\alpha_1} \left(\frac{p_{21}}{l_{21}} + \frac{p_{13} - p_{12}}{l_{23}} \right) - \frac{p_{13}^T P_{z_{12}} p_{13}}{l_{12} l_{13}^2 \sin\alpha_1} \\ &= \frac{1}{\sin\alpha_1} \left(-\frac{p_{12}^T P_{z_{13}} p_{12}}{l_{12} l_{13} l_{23}} - \frac{p_{12}^T P_{z_{13}} p_{12}}{l_{12}^2 l_{13}} - \frac{p_{13}^T P_{z_{12}} p_{13}}{l_{12} l_{13}^2} \right) \\ &= -\frac{\sin\alpha_1}{l_{12} l_{13} l_{23}} (l_{12}^2 + l_{12} l_{23} + l_{13} l_{23}) \end{aligned} \tag{20}$$

where $p_{ij} = p_j - p_i, i, j \in \mathcal{V}$. By using the law of sines $\frac{\sin\alpha_1}{l_{23}} = \frac{\sin\alpha_2}{l_{13}} = \frac{\sin\alpha_3}{l_{21}}$, one has

$$a_{11} = -\left(\frac{\sin\alpha_1}{l_{12}} + \frac{\sin\alpha_1}{l_{13}} + \frac{\sin\alpha_3}{l_{13}} \right) = -(g_1 + f_{13}) \tag{21}$$

where we define $f_{ij} = \frac{\sin\alpha_j}{l_{ij}}$, $g_i = (\sin\alpha_i) \left(\frac{1}{l_{i(i+1)}} + \frac{1}{l_{i(i-1)}} \right), i, j \in \{1, 2, 3\}$, and $(i-1) \in \mathcal{N}_i$, $(i+1) \in \mathcal{N}_i$.

Similarly, by using simplification and the law of sines, one also has

$$a_{22} = -\frac{\sin\alpha_2}{l_{12} l_{13} l_{23}} (l_{12}^2 + l_{12} l_{13} + l_{23} l_{13}) = -(g_2 + f_{23}). \tag{22}$$

Then, we calculate

$$\begin{aligned} a_{12} &= \left(\frac{p_{13}^T P_{z_{12}}}{l_{12} l_{13} \sin\alpha_1} + \frac{p_{12}^T P_{z_{13}}}{l_{12} l_{13} \sin\alpha_1} \right) \frac{p_{21} + p_{13}}{l_{23}} \\ &= \frac{l_{13}^2 - l_{12}^2 - \frac{p_{13}^T p_{12} p_{12}^T p_{13}}{l_{12}^2} + \frac{p_{12}^T p_{13} p_{13}^T p_{12}}{l_{13}^2}}{l_{12} l_{13} l_{23} \sin\alpha_1} \\ &= \frac{(l_{13}^2 - l_{12}^2) \sin\alpha_1}{l_{12} l_{13} l_{23}}. \end{aligned} \tag{23}$$

By using the law of sines $\frac{\sin\alpha_1}{l_{23}} = \frac{\sin\alpha_2}{l_{13}} = \frac{\sin\alpha_3}{l_{21}}$, one has

$$a_{12} = f_{12} - f_{13}. \tag{24}$$

Similarly, one has $a_{21} = \frac{(l_{23}^2 - l_{21}^2)\sin\alpha_2}{l_{12} l_{13} l_{23}} = f_{21} - f_{23}$. Note that the matrix $\tilde{F}_1$ is equal to F_s defined in [18].

Then, writing down all the other elements in matrix RB, one finds that RB has a block lower triangular structure. Consider that for agent $i, i \geq 4$, there are two desired angles $\alpha^*_{j_1 i j_2}$ and $\alpha^*_{j_2 i j_3}$ where $j_1, j_2, j_3 < i$ are the three neighboring agents whom the agent i will measure the directions with respect to. Then, one has (25) shown at the bottom of this page.

By using similar simplification as for the first three agents, one also has (26) shown at the bottom of this page.

Now, we find that $\tilde{F}_i, 4 \leq i \leq N$ in (26) is equal to F_i defined in [18]. By checking other matrix elements, one obtains that the matrix $R(X)B(X)$ in the closed-loop error dynamics (13) of double-integrators is the same as the system matrix $A(e_a)$ in the angle dynamics $\dot{e}_a = A(e_a) e_a$ of single-integrators (e_a denotes the column vector consisting of all the $2N-4$ independent angle errors), i.e.,

$$R(X)B(X) = A(e_a) = \begin{bmatrix} \tilde{F}_1 & 0 & 0 & \cdots & 0 \\ ** & \tilde{F}_4 & 0 & \cdots & 0 \\ ** & ** & \tilde{F}_5 & \cdots & 0 \\ \cdots & \cdots & \cdots & \ddots & \vdots \\ ** & ** & ** & ** & \tilde{F}_N \end{bmatrix} \tag{27}$$

which is an important and convenient fact for the later analysis. We summarize this using the following remark about matrices $\tilde{F}_i, i = 1, 4, \ldots, N$.

Remark 2: Under the angle set $\mathcal{A}$ and control law (8), $R(X)B(X)$ in the closed-loop error dynamics (13) of double-integrators is the same as the system matrix $A(e_a)$ in the dynamics $\dot{e}_a = A(e_a) e_a$ of single-integrators [18]. Therefore,

$$[RB]_{(2i-3:2i-4, 2i-3:2i-4)} = \tilde{F}_i = \begin{bmatrix} -(N_{j_1 i j_2} + N_{j_2 i j_1})(z_{i j_1} + z_{i j_2}) & -(N_{j_1 i j_2} + N_{j_2 i j_1})(z_{i j_2} + z_{i j_3}) \\ -(N_{j_2 i j_3} + N_{j_3 i j_2})(z_{i j_1} + z_{i j_2}) & -(N_{j_2 i j_3} + N_{j_3 i j_2})(z_{i j_2} + z_{i j_3}) \end{bmatrix}. \tag{25}$$

$$\tilde{F}_i = \begin{bmatrix} \bar{\omega}_1 & \bar{r}_{12} \\ \bar{r}_{21} & \bar{\omega}_2 \end{bmatrix} = \begin{bmatrix} -\sin\alpha_{j_1 i j_2} \left(\frac{1}{l_{i j_1}} + \frac{1}{l_{i j_2}} \right) & \frac{\sin\alpha_{j_2 i j_3}}{l_{i j_2}} - \frac{\sin\alpha_{j_1 i j_2} + \sin\alpha_{j_1 i j_3}}{l_{i j_1}} \\ \frac{\sin\alpha_{j_1 i j_2}}{l_{i j_2}} - \frac{\sin\alpha_{j_2 i j_3} + \sin\alpha_{j_1 i j_3}}{l_{i j_3}} & -\sin\alpha_{j_2 i j_3} \left(\frac{1}{l_{i j_3}} + \frac{1}{l_{i j_2}} \right) \end{bmatrix}. \tag{26}$$

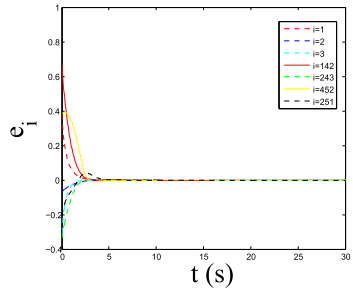

Fig. 3. Evolution of angle errors in Case 1.

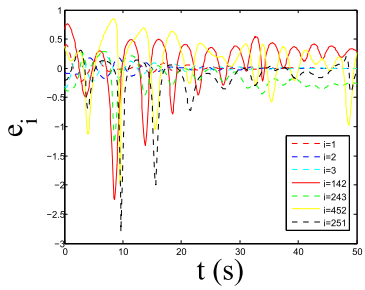

Fig. 4. Evolution of angle errors in Case 2.

according to [18, Thes. 7 and 8], the matrix $\tilde{F}_1^*$ is always Hurwitz and $\tilde{F}_i^* \quad \forall 4 \le i \le N$ are Hurwitz if Assumption 1 holds.

In the case of single-integrators, $A(e_a)|_{e_a=0}$ being Hurwitz is sufficient to make the formation's angle error dynamics $\dot{e}_a = A(e_a)e_a$ locally and exponentially stable. However, this is not sufficient for double-integrators due to (18). Note that in the case of double-integrators, according to (18) and (27), the necessary and sufficient condition to make (16) exponentially stable is that the solutions of

$$\det[\lambda(\lambda + k_s)I_2 - \tilde{F}_i^*] = 0, i = 1, 4, 5, \ldots, N \tag{28}$$

have negative real parts. While an arbitrary choice of positive gains does not make the single-integrator system unstable, this is not true for the double-integrator one as illustrated in the following simulation example.

Example 1: The desired angles: $\alpha_{123}^* = \pi/2, \alpha_{312}^* = \pi/4$, $\alpha_{231}^* = \pi/4, \alpha_{142}^* = \arctan(1.2), \alpha_{243}^* = \arctan(0.3), \alpha_{251}^* = \arctan(3/\sqrt{10}), \alpha_{452}^* = \arctan(1.2)$. The initial states: $p_1(0) = [0.5, 0.1]^T, p_2(0) = [0.1, 1.2]^T, p_3(0) = [-1.2, 0.2]^T$, $p_4(0) = [0.1, 2.0]^T, p_5(0) = [-1.4, 1.2]^T, \dot{p}_1(0) = [-0.1, -0.2]^T, \dot{p}_2(0) = [0.2, -0.1]^T, \dot{p}_3(0) = [-0.1, -0.1]^T$, $\dot{p}_4(0) = [-0.1, 0.4]^T, \dot{p}_5(0) = [0.1, 0.1]^T$.

Case 1: Single-integrator agent dynamics with Hurwitz matrices $\tilde{F}_i^*, i = 1, 4, 5$. The simulation result is shown in Fig. 3.

Case 2: Double-integrator agent dynamics with gain $k_s = 0.2$. The simulation result is shown in Fig. 4.

Example 1 illustrates that the proper selection of velocity damping gain k_s in angle-controlled double-integrator system is important. Now, we present the remaining results.

Lemma 1: Under Assumption 1, the matrix D_1^* is Hurwitz if and only if

$$k_s^2 Re(\lambda_{ij}) + (Im(\lambda_{ij}))^2 < 0, j = 1, 2 \tag{29}$$

holds for $\forall i = 1, 4, \ldots, N$, where λ_{i1} and λ_{i2} are the two conjugated eigenvalues of the matrix $\tilde{F}_i^*$, and *Re*() and *Im*() denote the real and imaginary parts of a complex number, respectively.

Proof: Note that one can always find a nonsingular matrix $\bar{P} \in \mathbb{C}^{2\times 2}$ such that

$$\tilde{F}_i^* = \bar{P} \begin{bmatrix} \lambda_{i1} & ** \\ 0 & \lambda_{i2} \end{bmatrix} \bar{P}^{-1} \tag{30}$$

where $**$ represents an element which does not affect the following analysis. Then, (28) can be written into

$$\begin{aligned} &\det[\lambda(\lambda + k_s)I_2 - \tilde{F}_i^*] \\ &= \det\left\{ \bar{P} \begin{bmatrix} \lambda(\lambda + k_s) - \lambda_{i1} & ** \\ 0 & \lambda(\lambda + k_s) - \lambda_{i2} \end{bmatrix} \bar{P}^{-1} \right\} \\ &= [\lambda(\lambda + k_s) - \lambda_{i1}][\lambda(\lambda + k_s) - \lambda_{i2}] \end{aligned} \tag{31}$$

which implies that the stability of (16) depends on the solutions of $\lambda(\lambda + k_s) - \lambda_{ij} = 0, i = 1, 4, \ldots, N, j = 1, 2$. Note that λ_{ij} can be a complex number. According to [26, Th. 40.1], (29) is the necessary and sufficient condition to guarantee that the two solutions of $\lambda(\lambda + k_s) - \lambda_{ij} = 0$ have negative real parts. □

Now, we further explore the condition (29) by calculating λ_{i1} and λ_{i2}. According to Lemma 1, we have that if Assumption 1 holds, then $A(e_a)|_{e_a=0} = R^* B^*$ is Hurwitz, which implies that $\mathrm{Re}(\lambda_{ij}) < 0, \forall i = 1, 4, \ldots, N, j = 1, 2$. According to Lemma 1, when $\mathrm{Im}(\lambda_{ij}) = 0, \lambda(\lambda + k_s) - \lambda_{ij} = 0$ will always have two solutions with negative real parts.

1) For the case of $\mathrm{Im}(\lambda_{i1}) = \mathrm{Im}(\lambda_{i2}) = 0$ in the first three agents, we require for $\tilde{F}_1^*$ in (19) that

$$\begin{aligned} \Delta_1^* &= (a_{11}^* - a_{22}^*)^2 + 4a_{12}^* a_{21}^* \\ &= (g_1^* + f_{13}^* - g_2^* - f_{23}^*)^2 + 4(f_{12}^* - f_{13}^*)(f_{21}^* - f_{23}^*) \ge 0. \end{aligned} \tag{32}$$

By using the law of sines $\frac{\sin\alpha_1^*}{l_{23}^*} = \frac{\sin\alpha_2^*}{l_{13}^*} = \frac{\sin\alpha_3^*}{l_{12}^*}$ and simplification, we can conclude that (32) can be written as

$$\begin{aligned} &\left(\frac{\sin\alpha_1^*}{\sin\alpha_2^*} + \frac{\sin\alpha_1^*}{\sin\alpha_3^*} + \frac{\sin\alpha_3^*}{\sin\alpha_2^*} - \frac{\sin\alpha_2^*}{\sin\alpha_1^*} - \frac{\sin\alpha_2^*}{\sin\alpha_3^*} - \frac{\sin\alpha_3^*}{\sin\alpha_1^*} \right)^2 \\ &+ 4\left(\frac{\sin\alpha_2^*}{\sin\alpha_3^*} - \frac{\sin\alpha_3^*}{\sin\alpha_2^*} \right)\left(\frac{\sin\alpha_1^*}{\sin\alpha_3^*} - \frac{\sin\alpha_3^*}{\sin\alpha_1^*} \right) \ge 0. \end{aligned} \tag{33}$$

Similarly for agents 4 to N, to guarantee $\mathrm{Im}(\lambda_{ij}) = 0, i = 4, \ldots, N, j = 1, 2$ for $\tilde{F}_i$ defined in (26), one has

$$\Delta_i^* = (\bar{\omega}_1^* - \bar{\omega}_2^*)^2 + 4\bar{r}_{12}^* \bar{r}_{21}^* \ge 0. \tag{34}$$

Multiplying $l_{ij_2}^{*2}$ at both sides of (34) and simplification yields

$$\begin{aligned} &\left[\left(\frac{\sin\alpha_{j_2 j_1 i}^*}{\sin\alpha_{ij_2 j_1}^*} + 1 \right) \sin\alpha_{j_1 i j_2}^* - \left(\frac{\sin\alpha_{ij_3 j_2}^*}{\sin\alpha_{ij_2 j_3}^*} + 1 \right) \sin\alpha_{j_2 i j_3}^* \right]^2 \\ &+ 4\left(\frac{\left(\sin\alpha_{j_1 i j_2}^* + \sin\alpha_{j_1 i j_3}^*\right)\sin\alpha_{j_2 j_1 i}^*}{\sin\alpha_{ij_2 j_1}^*} - \sin\alpha_{j_2 i j_3}^* \right) \end{aligned}$$

$$\times \left(\frac{(\sin\alpha^*_{j_2ij_3} + \sin\alpha^*_{j_1ij_3})\sin\alpha^*_{ij_3j_2}}{\sin\alpha^*_{ij_2j_3}} - \sin\alpha^*_{j_1ij_2} \right) \geq 0. \tag{35}$$

2) For the case of $\mathrm{Im}(\lambda_{ij}) \neq 0$, since $\mathrm{Im}(\lambda_{i1}) = -\mathrm{Im}(\lambda_{i2})$ and $\mathrm{Re}(\lambda_{i1}) = \mathrm{Re}(\lambda_{i2}) < 0$, the stability condition (29) can be written as

$$\Delta_i^* < 0 \ \ and \ \ 4k_s^2\mathrm{Re}(\lambda_{ij}) - \Delta_i^* < 0 \tag{36}$$

where $i = 1, 4, \ldots, N$, $j = 1, 2$, and $\mathrm{Re}(\lambda_{ij}) = \frac{a^*_{11}+a^*_{22}}{2}$ when $i = 1$ and $\mathrm{Re}(\lambda_{ij}) = \frac{\bar{\omega}^*_1+\bar{\omega}^*_2}{2}$ when $i \geq 4$. By combining the above two cases, one obtains the conditions such that all the eigenvalues of D_1^* have negative real parts, which implies that D_1^* is Hurwitz. In summary, we has the following result.

Proposition 1: Consider that N agents of double-integrator dynamics (1) are governed by (8) with the identical gain k_s, the initial errors $X(0)$ are sufficiently small, the initial inter-agent distances are bounded away from zero, and Assumption 1 holds. The system (13) is locally stable for $t \in [0, T_1)$ if (29) holds for $\forall i = 1, 4, \ldots, N$. Moreover, (29) holds if and only if for each $i = 1, 4, \ldots, N$, $\Delta_i^* \geq 0$ or (36) holds.

Note that if D_1^* is Hurwitz, $X = 0$ is the only equilibrium of (16), which is exponentially stable. We now analyze the evolution of the distance and angle errors among the agents to guarantee that the nonlinear closed-loop dynamics (13) is well-defined because the collinearity case $\sin\alpha_{jik} = 0, (j, i, k) \in \mathcal{A}$ and collision case $l_{ij} = 0, l_{ik} = 0$ will make (9) and (10) invalid, respectively. For $t \in [0, T_1)$, since D_1^* is Hurwitz, for an arbitrary positive definite matrix $Q_1 \in \mathbb{R}^{(4N-4)\times(4N-4)}$, there always exists a unique positive definite matrix $P_1 \in \mathbb{R}^{(4N-4)\times(4N-4)}$ such that

$$D_1^{*T}P_1 + P_1D_1^* = -Q_1. \tag{37}$$

Now, for system (16), we design the Lyapunov function candidate as

$$V_1 = X^TP_1X. \tag{38}$$

Taking the time-derivative of (38) yields

$$\dot{V}_1 = -X^TQ_1X \leq -\frac{\lambda_{\min}(Q_1)}{\lambda_{\max}(P_1)}V_1. \tag{39}$$

Then, it follows that:

$$\|X(t)\|^2 \leq \frac{V_1(t)}{\lambda_{\min}(P_1)} \leq \frac{V_1(0)}{\lambda_{\min}(P_1)}e^{-\frac{\lambda_{\min}(Q_1)}{\lambda_{\max}(P_1)}t}. \tag{40}$$

Since $\|X(t)\|^2 = e_1^2 + e_2^2 + e_{41}^2 + \cdots + e_{N1}^2 + e_{N2}^2 + \sum_{i=1}^N \|v_i\|^2$, one has that for $(j, i, k) \in \mathcal{A}$

$$|\alpha_{jik}(t) - \alpha^*_{jik}| \leq \|X(t)\| \leq \sqrt{\frac{V_1(0)}{\lambda_{\min}(P_1)}}e^{-\frac{\lambda_{\min}(Q_1)}{2\lambda_{\max}(P_1)}t} \tag{41}$$

$$\|v_i(t)\| \leq \|X(t)\| \leq \sqrt{\frac{V_1(0)}{\lambda_{\min}(P_1)}}e^{-\frac{\lambda_{\min}(Q_1)}{2\lambda_{\max}(P_1)}t}. \tag{42}$$

Note that (41) implies

$$\alpha^*_{jik} - \sqrt{\frac{V_1(0)}{\lambda_{\min}(P_1)}} \leq \alpha_{jik}(t) \leq \alpha^*_{jik} + \sqrt{\frac{V_1(0)}{\lambda_{\min}(P_1)}}. \tag{43}$$

According to (42), one has

$$\begin{aligned} l_{ij}(t) &= l_{ij}(0) + \int_0^t \dot{l}_{ij}(\tau)d\tau = l_{ij}(0) + \int_0^t z_{ij}^T(v_j - v_i)d\tau \\ &\geq l_{ij}(0) - \int_0^t (\|v_j\| + \|v_i\|)d\tau \\ &\geq l_{ij}(0) - 4\sqrt{\frac{V_1(0)}{\lambda_{\min}(P_1)}}\frac{\lambda_{\max}(P_1)}{\lambda_{\min}(Q_1)}(1 - e^{-\frac{\lambda_{\min}(Q_1)}{2\lambda_{\max}(P_1)}t}). \end{aligned} \tag{44}$$

Therefore, if

$$\alpha^*_{jik} > \sqrt{\frac{V_1(0)}{\lambda_{\min}(P_1)}} \ \text{ and } \ \alpha^*_{jik} + \sqrt{\frac{V_1(0)}{\lambda_{\min}(P_1)}} < \pi \tag{45}$$

then no collinearity happens among j, i, k. If

$$l_{ij}(0) > 4\sqrt{\frac{V_1(0)}{\lambda_{\min}(P_1)}}\frac{\lambda_{\max}(P_1)}{\lambda_{\min}(Q_1)} \tag{46}$$

no collision will happen between agents i and j.

Because α^*_{jik} is bounded away from zero and π, and $l_{ij}(0)$ is bounded away from zero, and $X(0), V_1(0)$ are sufficiently small, (45) and (46) hold for $t \in [0, T_1)$. Assume that there exists a collision or collinearity in $[T_1, \infty)$ and denote the first time that it happens by T_2^-. Then, one has the following two cases.

1) Collision between i and j happens at T_2^-: Since no collision and collinearity happens in $[0, T_2^-)$, the closed-loop system is well-defined in $[0, T_2^-)$. Following the calculations in (38)–(44), one has that

$$l_{ij}(T_2^-) \geq l_{ij}(0) - 4\sqrt{\frac{V_1(0)}{\lambda_{\min}(P_1)}}\frac{\lambda_{\max}(P_1)}{\lambda_{\min}(Q_1)} > 0$$

which is bounded away from zero. This implies a contradiction with the assumption that collision happens at T_2^-. Thus, no collision between agents i and j happens at T_2^-.

2) Collinearity among j, i, k happens at T_2^-: Then, one has that $\alpha_{jik}(T_2^-)$ will approach zero or π. Since no collinearity and collision happens in $[0, T_2^-)$, using (43), one has that $\alpha_{jik}(T_2^-)$ is bounded away from zero and π which implies a contradiction. Therefore, no collinearity will occur among j, i, k at T_2^-.

Since none of the above two cases is possible, no collision and collinearity will happen in $[0, \infty)$ given that the initial formation is sufficiently close to the desired formation, i.e., $V_1(0)$ is sufficiently small. Then, the system (13) is well-defined from $t = 0$ to $+\infty$, under which the asymptotic stability can be established by using the same analysis from (9)–(36) for $\forall t \in [0, \infty)$. The following theorem summarizes the main result.

Theorem 1: Consider that N agents of double-integrator dynamics (1) are governed by (8) with the identical gain k_s, the initial errors $X(0)$ are sufficiently small, the initial distances are

bounded away from zero, and Assumption 1 holds. The formation stabilization defined in (2)–(5) is locally and asymptotically achieved for $t \geq 0$ if (29) holds for $\forall i = 1, 4, \ldots, N$.

Remark 3: Since the initial angles in Example 1 are close to the desired angles, we can use the initial states given in Example 1 to approximately check the stability of the formations governed by the single-integrator agent dynamics and the double-integrator agent dynamics, respectively.

B. Case of Distinct Control Gains

The designed formation stabilization law (8) in the previous section requires all the agents to have the identical velocity feedback gains k_s. To adapt for different actuator characteristics, e.g., speed constraints in different agents, in this section we design a formation stabilization law which allows each agent to have distinct control gain k_i, namely, the control input for agent $i, i = 1, \ldots, N$ is given by

$$u_i = -k_i v_i - \sum\nolimits_{(j,i,k)\in\mathcal{A}} (\alpha_{jik} - \alpha^*_{jik})(z_{ij} + z_{ik}) \quad (47)$$

where $k_i > 0$ and k_i can be different from k_j. By choosing the same system state variable X in (12), one has the closed-loop dynamics of X

$$\dot{X} = \begin{bmatrix} 0_{(2N-4)\times(2N-4)} & R(X) \\ B(X) & -\text{diag}\{k_i\} \otimes I_2 \end{bmatrix} X = D_2(X)X \quad (48)$$

where $\text{diag}\{k_i\} = \text{diag}\{k_1, \ldots, k_N\} \in \mathbb{R}^{N\times N}$. To prove the local stability of (48), we consider the characteristic polynomial of D_2^* again, that is

$$|\lambda I_{4N-4} - D_2^*| = \begin{vmatrix} \lambda I_{2N-4} & -R^* \\ -B^* & \text{diag}\{\lambda + k_i\} \otimes I_2 \end{vmatrix} \quad (49)$$

where $\text{diag}\{\lambda + k_i\} = \text{diag}\{\lambda + k_1, \ldots, \lambda + k_N\}$. According to Schur complement theorem, one has

$$|\lambda I_{4N-4} - D_2^*| = \prod_{i=1}^{N} \{(\lambda + k_i)\text{det}[\lambda I_{2N-4} - R^* \text{diag}\{(\lambda + k_i)^{-1}\} \otimes I_2 B^*]\}.$$

By multiplying matrix B^* with $\text{diag}\{(\lambda + k_i)^{-1}\} \otimes I_2$ then with matrix R^*, it can be observed that

$$R^*\text{diag}\{(\lambda + k_i)^{-1}\} \otimes I_2 B^* = \begin{bmatrix} \bar{F}_1^* & 0 & 0 & \cdots & 0 \\ ** & \frac{\tilde{F}_4^*}{\lambda+k_4} & 0 & \cdots & 0 \\ ** & ** & \frac{\tilde{F}_5^*}{\lambda+k_5} & \cdots & 0 \\ \cdots & \cdots & \cdots & \ddots & \vdots \\ ** & ** & ** & ** & \frac{\tilde{F}_N^*}{\lambda+k_N} \end{bmatrix} \quad (50)$$

where $\bar{F}_1^* = \bar{F}_1(X)|_{X=0}$, $\bar{F}_1(X) = \begin{bmatrix} \tilde{a}_{11} & \tilde{a}_{12} \\ \tilde{a}_{21} & \tilde{a}_{22} \end{bmatrix}$ and

$$\tilde{a}_{11} = \frac{(N_{213} + N_{312})(-z_{12} - z_{13})}{\lambda + k_1} + \frac{N_{213}(z_{31} + z_{32})}{\lambda + k_3}$$

$$\tilde{a}_{12} = \frac{N_{312}(z_{21} + z_{23})}{\lambda + k_2} + \frac{N_{213}(z_{31} + z_{32})}{\lambda + k_3},$$

$$\tilde{a}_{21} = \frac{(N_{321} + N_{123})(-z_{21} - z_{23})}{\lambda + k_2} + \frac{N_{123}(z_{31} + z_{32})}{\lambda + k_3}$$

$$\tilde{a}_{22} = \frac{(N_{321} + N_{123})(-z_{21} - z_{23})}{\lambda + k_2} + \frac{N_{123}(z_{31} + z_{32})}{\lambda + k_3}.$$

Then, it follows that:

$$|\lambda I_{4N-4} - D_2^*| = \left\{\prod_{i=1}^{3}(\lambda + k_i)\right\} \text{det}(\lambda I_2 - \bar{F}_1^*) \times \left\{\prod_{i=4}^{N} \text{det}[\lambda(\lambda + k_i) I_2 - \tilde{F}_i^*]\right\}. \quad (51)$$

Note that the stability condition of $\{\prod_{i=4}^{N} \text{det}[\lambda(\lambda + k_i)I_2 - \tilde{F}_i^*]\} = 0$ obtained from (51) is the same as (28), which implies that there is no difference for the stability condition when agents 4 to N have identical or distinct velocity damping gains. Then, the stability condition for agents 4 to N can also be described as

$$k_i^2 \text{Re}(\lambda_{ij}) + (\text{Im}(\lambda_{ij}))^2 < 0, i = 4, \ldots, N, j = 1, 2 \quad (52)$$

which holds when (35) or (36) hold for $i = 4, \ldots, N$. But this is not the case for the first three agents. For the first three agents, different from (28), the corresponding element in $\{\prod_{i=1}^{3}(\lambda + k_i)\}(\lambda I_2 - \bar{F}_1^*) = \begin{bmatrix} \bar{a}_{11}^* & \bar{a}_{12}^* \\ \bar{a}_{21}^* & \bar{a}_{22}^* \end{bmatrix}$ becomes that

$$\begin{aligned} \bar{a}_{11}^* = & [\lambda(\lambda + k_1)(\lambda + k_2)(\lambda + k_3) \\ & - (N_{213} + N_{312})(-z_{12} - z_{13})(\lambda + k_2)(\lambda + k_3) \\ & - N_{213}(z_{31} + z_{32})(\lambda + k_1)(\lambda + k_2)]|_{X=0} \\ \bar{a}_{22}^* = & [\lambda(\lambda + k_1)(\lambda + k_2)(\lambda + k_3) \\ & - (N_{321} + N_{123})(-z_{21} - z_{23})(\lambda + k_1)(\lambda + k_3) \\ & - N_{123}(z_{31} + z_{32})(\lambda + k_1)(\lambda + k_2)]|_{X=0} \\ \bar{a}_{12}^* = & -[N_{312}(z_{21} + z_{23})(\lambda + k_1)(\lambda + k_3) \\ & - N_{213}(z_{31} + z_{32})(\lambda + k_1)(\lambda + k_2)]|_{X=0} \\ \bar{a}_{21}^* = & -[(N_{321} + N_{123})(-z_{21} - z_{23})(\lambda + k_1)(\lambda + k_3) \\ & - N_{123}(z_{31} + z_{32})(\lambda + k_1)(\lambda + k_2)]|_{X=0}. \end{aligned}$$

By letting $\{\prod_{i=1}^{3}(\lambda + k_i)\}\text{det}(\lambda I_2 - \bar{F}_1^*) = 0$, the stability condition of the first three agents becomes that the eight solutions of the following algebraic equation all have negative real parts:

$$\bar{a}_{11}^* \bar{a}_{22}^* - \bar{a}_{12}^* \bar{a}_{21}^* = b_8\lambda^8 + b_7\lambda^7 + \cdots + b_1\lambda + b_0 = 0 \quad (53)$$

which can be checked by Routh stability criterion [26, Th. 40.1] or some numerical tools (e.g., MATLAB). But the explicit solution of (53) is hard to be obtained due to the high order of (53). The algebraic equation (53) is related to the desired triangular formation shape and the velocity damping gains k_1, k_2, k_3, which implies that an inappropriate selection of the first three agents' velocity damping gains may cause the system unstable.

Finally, we summarize the above discussion into the following result.

Theorem 2: Consider that N agents governed by (47) with distinct gains k_i, the initial errors $X(0)$ are sufficient small, initial inter-agent distances are bounded away from zero and Assumption 1 holds. The formation stabilization defined in (2)–(5) can be locally achieved if all the solutions of (53) have negative real parts and (52) holds. Moreover, (52) holds if and only if for each $i = 4, \ldots, N$, (35) or (36) holds.

The proof of theorem is followed by the above analysis. The analysis of collision and collinearity is similar to Theorem 1.

Remark 4: The formation stabilization laws (8) and (47) can be implemented in each agent's local coordinate frame, i.e., the alignment of all agents' local coordinate frames is not needed. This can be obtained straightforwardly by following [18, Remark 6].

IV. Formation Maneuvering

Different from the case of formation stabilization, the maneuvering of angle rigid formations requires all agents to not only achieve the desired formation shape, but also move with the desired collective motion in terms of translation, rotation and scaling. Because of the cascading construction of the desired angle rigid formation in Section II-C, the rotational and scaling maneuvering can be controlled by the first triangular formation formed by the first three agents. According to (7), given a nonzero desired relative position $\delta_{13}^*(t)$ from agent 1 to agent 3, the desired orientation and scale of the formation can be determined by $\delta_{13}^*(t)/\|\delta_{13}^*(t)\|$ and $\|\delta_{13}^*(t)\|$, respectively. Therefore, the objective of this section is to achieve the desired angles, the same translational maneuvering velocity $v_c^*(t) \in \mathbb{R}^2$ for all the agents, and maintain the desired relative position $\delta_{13}^*(t)$ from agent 1 to agent 3. Let $\{t_1, t_2, \ldots, t_n\}$ be the instants that $\delta_{13}^*(t)$ switches its values where $n \in \mathbb{N}^+$. Then, we present the assumption on the change of $\delta_{13}^*(t)$.

Assumption 2: Each agent has the knowledge of $v_c^*, \dot{v}_c^*$. The desired relative position $\delta_{13}^*(t)$ satisfies three properties: 1) $\delta_{13}^*(t)$ is piecewise-constant and bounded, and $\dot{\delta}_{13}^*(t) \neq 0 \quad \forall t > 0$; 2) the number of its abrupt jumps is finite; 3) the neighboring change of $\delta_{13}^*(t)$ is bounded and sufficiently small, i.e., $\|\delta_{13}^*(t_i^-) - \delta_{13}^*(t_i^+)\| \leq \varepsilon \quad \forall i = 1, 2, \ldots, n$ where ε is a positive and small number.

Remark 5: The agents can either communicate or employ a consensus-based finite-time estimator to obtain v_c^* and $\dot{v}_c^*$. Compared to the previously proposed maneuvering pattern [19], [27] where the rotational or scaling maneuvering speed is constant for all time, the maneuvering pattern defined in this article is more practical since $\delta_{13}^*(t)$ only needs to be changed when the rotational or scaling maneuvering is necessary for the execution of the current task. Moreover, the requirement that ε should be sufficiently small can be fulfilled in practice by changing $\delta_{13}^*(t)$ with longer time t_n and more steps n. This is equivalent to requiring that the rotational and scaling speed should not be very large, which is similarly needed in [11], [19], and [27].

Now, we design the formation maneuvering algorithm to be

$$u_i(t) = \dot{v}_c^*(t) - k_s(v_i(t) - v_c^*) - k_{mi}(p_3(t) - p_1(t) - \delta_{13}^*(t)) - \sum\nolimits_{(j,i,k)\in\mathcal{A}} (\alpha_{jik}(t) - \alpha_{jik}^*)(z_{ij}(t) + z_{ik}(t)) \tag{54}$$

where $k_{mi} = 1$ if $i = 3$, and $k_{mi} = 0$ otherwise. First, we analyze the convergence of the formation within the time interval $t \in [0, t_1]$ where $\delta_{13}^*(t)$ is constant. We need to obtain the angle error dynamics, velocity error dynamics, and the relative position error dynamics of the closed-loop system under the designed maneuvering algorithm (54). In this maneuvering case, we define the system state variables

$$Y = [e_1, e_2, e_{41}, e_{42}, \ldots, e_{N1}, e_{N2}, \tilde{p}_{13}^T, v_1^T - v_c^{*T}, \ldots, v_N^T - v_c^{*T}]^T \tag{55}$$

where $\tilde{p}_{13} = p_3 - p_1 - \delta_{13}^*$ and $Y \in \mathbb{R}^{4N-2}$. Our objective is to prove that $Y = 0$ is a locally stable equilibrium under (54). Similar to the formation stabilization case, $\ddot{p}_i(0)$ is bounded if the initial velocity $v_i(0)$ is bounded and $l_{ij}(0), l_{ik}(0), \sin\alpha_{jik}(0)$ are bounded away from zero. Therefore, $\exists T_2 > 0, T_2 \leq t_1$ such that $l_{ij}(t), l_{ik}(t), \sin\alpha_{jik}(t) \quad \forall (j,i,k) \in \mathcal{A}$ are bounded away from zero for $t \in [0, T_2)$. We first analyze the error dynamics for $t \in [0, T_2)$. According to (11), one has

$$\begin{aligned}\dot{\alpha}_{jik} = & -z_{ik}^T \frac{P_{z_{ij}}}{l_{ij}\sin\alpha_{jik}} v_j - z_{ij}^T \frac{P_{z_{ik}}}{l_{ik}\sin\alpha_{jik}} v_k \\ & + (z_{ik}^T \frac{P_{z_{ij}}}{l_{ij}\sin\alpha_{jik}} + z_{ij}^T \frac{P_{z_{ik}}}{l_{ik}\sin\alpha_{jik}}) v_i.\end{aligned} \tag{56}$$

Note that the velocity error variable in this case is $v_i - v_c^*$ instead of v_i. Therefore, we rewrite (56) into

$$\begin{aligned}\dot{\alpha}_{jik} = & -z_{ik}^T \frac{P_{z_{ij}}}{l_{ij}\sin\alpha_{jik}} (v_j - v_c^*) - z_{ij}^T \frac{P_{z_{ik}}}{l_{ik}\sin\alpha_{jik}} (v_k - v_c^*) \\ & + \left(z_{ik}^T \frac{P_{z_{ij}}}{l_{ij}\sin\alpha_{jik}} + z_{ij}^T \frac{P_{z_{ik}}}{l_{ik}\sin\alpha_{jik}} \right) (v_i - v_c^*) \\ & - z_{ik}^T \frac{P_{z_{ij}}}{l_{ij}\sin\alpha_{jik}} v_c^* - z_{ij}^T \frac{P_{z_{ik}}}{l_{ik}\sin\alpha_{jik}} v_c^* \\ & + \left(z_{ik}^T \frac{P_{z_{ij}}}{l_{ij}\sin\alpha_{jik}} + z_{ij}^T \frac{P_{z_{ik}}}{l_{ik}\sin\alpha_{jik}} \right) v_c^*.\end{aligned} \tag{57}$$

In the following, we investigate the effect of the translational maneuvering term v_c^* on the angle dynamics $\dot{\alpha}_{jik}$ in (57). Note that

$$\begin{aligned}& - z_{ik}^T \frac{P_{z_{ij}}}{l_{ij}\sin\alpha_{jik}} v_c^* - z_{ij}^T \frac{P_{z_{ik}}}{l_{ik}\sin\alpha_{jik}} v_c^* \\ & + \left(z_{ik}^T \frac{P_{z_{ij}}}{l_{ij}\sin\alpha_{jik}} + z_{ij}^T \frac{P_{z_{ik}}}{l_{ik}\sin\alpha_{jik}} \right) v_c^* = 0.\end{aligned} \tag{58}$$

Therefore, (57) and (58) imply that the translational maneuvering has no effect on the angle dynamics $\dot{\alpha}_{jik}, (j,i,k) \in \mathcal{A}$ in (57). This is because the whole formation's translation will not change the interior angle α_{jik}. Therefore, one still has the

similar angle dynamics $\dot{\alpha}_{jik}$ in (57) as the case of formation stabilization (10).

Then, we analyze the velocity error dynamics of $v_i - v_c^*$. Using (54), one has

$$\dot{v}_i - \dot{v}_c^* = -k_s(v_i - v_c^*) - k_{mi}(p_3 - p_1 - \delta_{13}^*) - \sum\nolimits_{(j,i,k)\in\mathcal{A}} (\alpha_{jik} - \alpha_{jik}^*)(z_{ij} + z_{ik}).$$

The dynamics of the relative position errors can be described by

$$\dot{\tilde{p}}_{13} = v_3 - v_c^* - (v_1 - v_c^*). \tag{59}$$

Summarizing (57)–(59) yields the overall dynamics

$$\dot{Y} = \begin{bmatrix} 0_{(2N-4)\times(2N-4)} & 0 & R(Y) \\ 0 & 0_{2\times 2} & K_2 \\ B(Y) & K_1 & -k_s I_{2N} \end{bmatrix} Y = D_3(Y)Y \tag{60}$$

where $R(Y)$ and $B(Y)$ have the same definitions as (14) and (15), respectively, $K_1 = [0_{2\times2}; 0_{2\times2}; -I_2; 0_{2\times2}; \ldots; 0_{2\times2}] \in \mathbb{R}^{2N\times 2}$ and $K_2 = [-I_2, 0_{2\times2}, I_2, 0_{2\times2}, \ldots, 0_{2\times2}] \in \mathbb{R}^{2\times 2N}$. Using a similar linearization step for (60) as (13)–(16), the linearized dynamics of (60) around the desired equilibrium $Y = 0$ can be described by

$$\dot{Y} = \begin{bmatrix} 0_{(2N-4)\times(2N-4)} & 0 & \bar{R}^* \\ 0 & 0_{2\times 2} & K_2 \\ \bar{B}^* & K_1 & -k_s I_{2N} \end{bmatrix} Y = D_3^* Y \tag{61}$$

where $\bar{R}^* = R(Y)|_{Y=0}$ and $\bar{B}^* = B(Y)|_{Y=0}$ can be different from R^* and B^*, respectively, due to the different interagent distances at their equilibrium points. Following the calculation method in (18), the characteristic polynomial of D_3^* can be written as (62) shown at the bottom of the this page. According to the definitions of K_1 and K_2, one has

$$\bar{R}^* K_1 K_2 \bar{B}^* = \begin{bmatrix} \hat{F}_1^* & 0 & \cdots & 0 \\ ** & 0 & \cdots & 0 \\ ** & ** & \ddots & 0 \\ ** & ** & \cdots & 0 \end{bmatrix}$$

$$\hat{F}_1^* = \begin{bmatrix} N_{213}^*(z_{32}^* + z_{12}^*) & N_{213}^* z_{32}^* \\ N_{123}^* z_{12}^* & N_{123}^* z_{31}^* \end{bmatrix} \tag{63}$$

where $**$ in the matrix $\bar{R}^* K_1 K_2 \bar{B}^*$ represents some elements that will not affect the following analysis. According to the matrix structure in (62) and (63), one has that compared to the dynamics (16), the dynamics of $\tilde{p}_{13}$ in (61) only affect the angle error dynamics of the first three agents, and does not affect the remaining agents' angle error dynamics. Using the fact $(\lambda^2 + k_s\lambda + 1)^2 = \det(\mathrm{diag}[\lambda^2 + k_s\lambda + 1, \lambda^2 + k_s\lambda + 1, 1, \ldots, 1])$ for (62), one has

$$|\lambda I_{4N-2} - D_3^*| = (\lambda + k_s)^2 \{\prod_{i=4}^{N} \det[\lambda(\lambda + k_i)I_2 - \tilde{F}_i^*]\} \times \det\{(\lambda^2 + k_s\lambda + 1)[\lambda(\lambda + k_s)I_2 - \tilde{F}_1^*] - \hat{F}_1^*\}. \tag{64}$$

Therefore, D_3^* has two eigenvalues $-k_s, -k_s$, and $4(N-3)$ eigenvalues lying in $\prod_{i=4}^{N} \det[\lambda(\lambda + k_i)I_2 - \tilde{F}_i^*]\} = 0$, and 8 eigenvalues lying in $\det\{(\lambda^2 + k_s\lambda + 1)[\lambda(\lambda + k_s)I_2 - \tilde{F}_1^*] - \hat{F}_1^*\} = 0$. Now, we are ready to present the main result.

Theorem 3: Consider that N agents of double-integrator agent dynamics (1) are governed by (54), the initial angle and velocity errors are sufficiently small, the initial interagent distances are bounded away from zero, Assumption 1 holds and $t \in [0, t_1]$. The formation maneuvering errors defined in (3)–(7) will locally and exponentially converge if Assumption 2 and (29) hold for $i = 4, \ldots, N$, and the solutions of $\det\{(\lambda^2 + k_s\lambda + 1)[\lambda(\lambda + k_s)I_2 - \tilde{F}_1^*] - \hat{F}_1^*\} = 0$ have negative real parts.

Proof: Under the assumptions in Theorem 3, all the eigenvalues of D_3^* have negative real parts, which implies the local and exponential stability of (60) when $t \in [0, T_2)$. Now, we extend T_2 to t_1 to establish the stability of (60) for $t \in [0, t_1]$. First, one can construct a Lyapunov function $V_2 = Y^T P_2 Y$ where $P_2 = P_2^T > 0$ satisfying $D_3^{*T} P_2 + P_2 D_3^* = -Q_2 < 0$. Similar to (38)–(45), one has that no collinearity will happen since (41) and (45) still hold. The analysis for the distance change l_{ij} is slightly different. Note that (42) is changed to

$$\|v_i - v_c^*\| \le \|Y(t)\| \le \sqrt{\frac{V_2(0)}{\lambda_{\min}(P_2)}} e^{-\frac{\lambda_{\min}(Q_2)}{2\lambda_{\max}(P_2)}t}. \tag{65}$$

$$\begin{aligned} |\lambda I_{4N-2} - D_3^*| &= \begin{vmatrix} \lambda I_{(2N-4)} & 0 & -\bar{R}^* \\ 0 & \lambda I_2 & -K_2 \\ -\bar{B}^* & -K_1 & (\lambda + k_s)I_{2N} \end{vmatrix} \\ &= (\lambda + k_s)^2 \det\left(\lambda(\lambda + k_s)I_{2N-2} - \begin{bmatrix} \bar{R}^*\bar{B}^* & \bar{R}^* K_1 \\ K_2\bar{B}^* & K_2 K_1 \end{bmatrix}\right) \\ &= (\lambda + k_s)^2 \det \begin{bmatrix} \lambda(\lambda + k_s)I_{2N-4} - \bar{R}^*\bar{B}^* & -\bar{R}^* K_1 \\ -K_2\bar{B}^* & (\lambda^2 + k_s\lambda + 1)I_2 \end{bmatrix} \\ &= (\lambda + k_s)^2(\lambda^2 + k_s\lambda + 1)^2 \\ &\quad \times \det[\lambda(\lambda + k_s)I_{2N-4} - \bar{R}^*\bar{B}^* - \frac{\bar{R}^* K_1 K_2 \bar{B}^*}{\lambda^2 + k_s\lambda + 1}]. \end{aligned} \tag{62}$$

Also, (44) is changed to

$$l_{ij}(t) = l_{ij}(0) + \int_0^t z_{ij}^T (v_j - v_i) d\tau$$
$$\geq l_{ij}(0) - \int_0^t (\|v_j - v_c^*\| + \|v_i - v_c^*\|) d\tau$$
$$\geq l_{ij}(0) - 4\sqrt{\frac{V_2(0)}{\lambda_{\min}(P_2)}} \frac{\lambda_{\max}(P_2)}{\lambda_{\min}(Q_2)} (1 - e^{-\frac{\lambda_{\min}(Q_2)}{2\lambda_{\max}(P_2)} t}). \quad (66)$$

Therefore, if $l_{ij}(0) > 4\sqrt{\frac{V_2(0)}{\lambda_{\min}(P_2)}} \frac{\lambda_{\max}(P_2)}{\lambda_{\min}(Q_2)}$, then $l_{ij}(t) > 0$. Since $V_2(0)$ is sufficiently small and $l_{ij}(0)$ is bounded away from zero, T_2 can be extended to t_1. Then, it follows that $\lim_{t\to\infty} Y(t) = 0$, which implies that the formation maneuvering errors defined in (3)–(7) will be locally and exponentially converge for $t \in [0, t_1]$. By summarizing the above analysis, we come to the conclusion that the transnational formation maneuvering and desired constant relative position δ_{12}^* are achieved under (54) for $t \in [0, t_1]$. □

Now, we discuss the case where $t \in [0, \infty)$ and $\delta_{12}^*(t)$ is piecewise-constant. Since the control input $u_i(t)$ in (54) is piecewise-continuous, the integration of $u_i(t)$, i.e., agent i's velocity $v_i(t)$, is continuous, which implies that the evolution of velocity error $v_i - v_c^*(t)$ is also continuous. Also, the integration of $v_i(t)$, i.e., agent i's position $p_i(t)$, is continuous, which implies that the evolution of angle error $\alpha_{jik} - \alpha_{jik}^*, \{j, k\} \in \mathcal{N}_i$ is also continuous. Therefore, under Assumption 2, both the velocity errors and the angle errors converge to zero. For the relative position error, one has

$$\|\tilde{p}_{13}(t_i^+) - \tilde{p}_{13}(t_i^-)\|$$
$$= \|p_{13}(t_i^+) - \delta_{12}^*(t_i^+) - p_{13}(t_i^-) + \delta_{12}^*(t_i^-)\|$$
$$= \|\delta_{13}^*(t_i^+) - \delta_{13}^*(t_i^-)\| \leq \varepsilon \quad (67)$$

where $i = 1, 2, .., n$ and we have used the fact that $p_{13}(t_i^+) = p_{13}(t_i^-)$ since $p_1(t), p_3(t)$ are continuous. Using Assumption 2, one has that $\|\tilde{p}_{13}(t_i^+) - \tilde{p}_{13}(t_i^-)\|$ is sufficiently small. Therefore, if $\tilde{p}_{13}(0)$ is sufficiently small, then $\tilde{p}_{13}(t_i^+), \forall i = 1, \ldots, n$ is sufficiently small. Then, for each $t \in [t_i, t_{i+1}]$, one can always employ a similar analysis from (60)–(66) to obtain the convergence of $Y(t)$ within $t \in [t_i, t_{i+1}]$. Since the number of abrupt jump of $\delta_{13}(t)$ is finite, one has that after the final jump at $t = t_n$, $Y(t)$ will converge to zero as $t \to \infty$.

Remark 6: In the stabilization of distance rigid formations with double-integrator agent dynamics [13], the fact that their control law is the gradient of a potential function helps their stability analysis, see, e.g., the multiplication of rigidity matrix and its transpose being positive semidefinite, and a nice structure in the Jacobian matrix of the linearized system. However, for the control law (8) designed for the stabilization of angle rigid formations with double-integrator agent dynamics, it can be proved that it is not a gradient-based control law due to the asymmetric/directed direction measurements, which makes its stability analysis challenging and this work essential. One of the main contributions of this article is the finding that the relationship between single-integrator and double-integrator agent dynamics for angle rigid formations is underscored by $R(p)B(p) = A(e_a)$ obtained in (27). In addition, according to the local unique determination in Remark 1, the nonlinear dynamics (13) is indeed not globally stable.

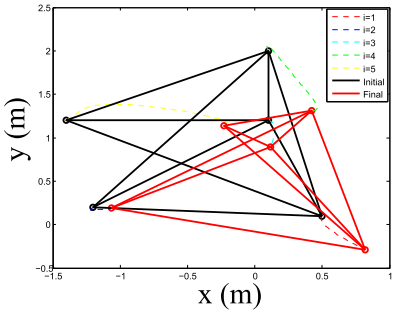

Fig. 5. Formation stabilization trajectories.

Remark 7: To implement the formation maneuvering laws (54) and (54) according to all the agents' local coordinate frames, the desired translational maneuvering velocity v_c^* needs to be described in each agent's local coordinate frame in the design stage. But this is not required for rotation and scaling maneuverings since δ_{13}^* can be described in agent 3's local coordinate frame. In addition, given the desired angles and δ_{13}^*, the solutions of $\det\{(\lambda^2 + k_s\lambda + 1)[\lambda(\lambda + k_s)I_2 - \tilde{F}_1^*] - \hat{F}_1^*\} = 0$ in Theorem 3 can be checked. The reason we choose to control the relative position between agents 1 and 3 instead of agents 1 and 2 or agents 2 and 3 is that in the Step 2 of constructing the desired formation, we select the combination of angles $\alpha_{142}, \alpha_{243}$, under which the edges 12 and 23 lie inside $\triangle 143$, and the edge 13 lies in the outer boundary of $\triangle 143$. Although, controlling arbitrary one of these three edges can guarantee the closed-loop dynamics stable, simulation examples show that controlling the edge 13 comes with smaller overshoot than controlling the other two edges. We will consider the optimal selection of the controlling edge as our future work.

V. Simulation Examples

We use numerical simulation examples to illustrate the effectiveness of the proposed formation stabilization and maneuvering control algorithms.

A. Formation Stabilization

The simulation parameters including agents' initial states and desired angles are the same as those given in Example 1 of Section IV. It can be checked that the stability condition (29) holds when the identical velocity damping gain is chosen as $k_s = 2$.

Under the formation control law (8) with $k_s = 2$, the simulation results are shown in Figs. 5 and 6. According to the formation stabilization trajectories shown in Fig. 5, the desired angle rigid formation is achieved. According to the evolution of angle errors shown in Fig. 6, all the angle errors converge to zero within 20 s, in which the maximum initial angle error is 0.7.

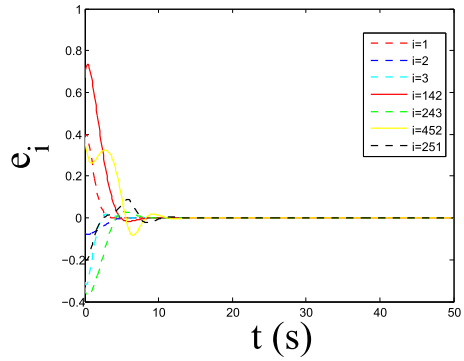

Fig. 6. Angle errors in formation stabilization.

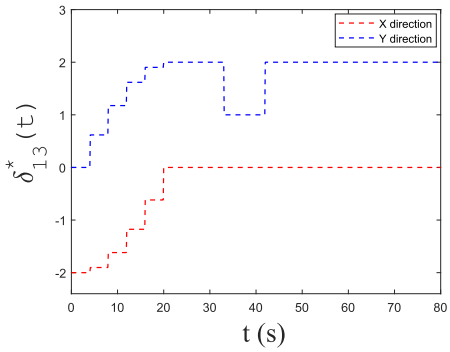

Fig. 7. Change of piecewise-constant $\delta^*_{13}(t)$.

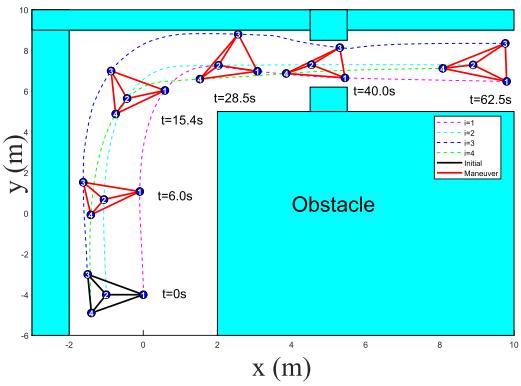

Fig. 8. Formation maneuvering trajectories when conducting the exploration of the unknown environment.

B. Formation Maneuvering

We consider the formation maneuvering of four agents to achieve the exploration of an unknown environment. The agents' desired angles are the same as those given in the simulation part of [27]. The agents' initial states are chosen as $p_1(0)=[0;-4], p_2(0)=[-1;-4], \dot{p}_3(0)=[-1.5;-3]$, $p_4(0)=[-1.4;-4.9], \dot{p}_1(0)=[0.1;-0.1], \dot{p}_2(0)=[0.1;-0.1]$, $\dot{p}_3(0)=[-0.1;0.1], \dot{p}_4(0)=[-0.1;0.1]$. The control gain is selected as $k_s=10$. The desired translational velocity is selected as: $v_c^*(t)=[0;0.82], t\in[0,4]; v_c^*(t)=[0.05*t; 0.82-0.82(t-4)/20], t\in[4,24]; v_c^*(t)=[0.2;0], t>24$. The piecewise-constant $\delta^*_{13}(t)$ is shown in Fig. 7. Under the control law (54), the maneuvering trajectories and the evolution of angle errors are shown in Figs. 8 and 9, respectively.

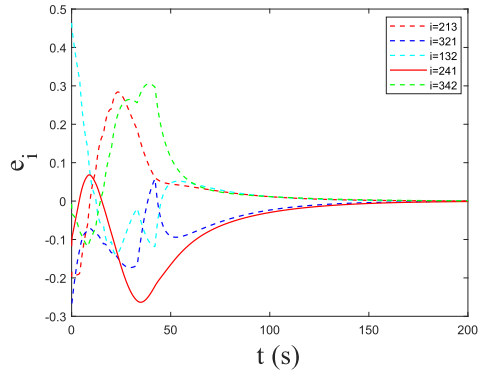

Fig. 9. Evolution of angle errors.

According to Figs. 7–9, one sees that the formation maneuvering with translation, rotation and scaling is achieved under the proposed law (54). Although, $\delta^*_{13}(t)$ is piecewise-constant in Fig. 7, the angle errors in Fig. 9 are continuous, and converge to zero at 150 s after the final scaling maneuvering at 42 s. According to Fig. 7, the formation rotates by $\pi/2$ from 4 to 24 s, and shrinks to half of the original formation at 33 s, which demonstrates the effectiveness of the proposed maneuvering approach. Compared to the the maneuvering approach for single-integrators in [11] and [27], a specified rotating angle and scaling size can be achieved in this approach.

VI. Conclusion

This article has designed control algorithms to stabilize and maneuver angle rigid formations governed by double-integrator dynamics. For the stabilization case, each agent only needs to measure its own velocity and directions with respect to its neighbors. The proposed formation stabilization control law can be implemented in agents' local coordinate frames, i.e., the alignment of agents' coordinate frames is not needed. For the maneuvering case, in addition to the sensor measurements required in the stabilization case, one of the first three agents must measure its relative position with respect to the maneuvering reference agent such that the desired translational, rotational, and scaling maneuvering can be achieved. Compared to the single-integrator agents, the stabilization and maneuvering of double-integrators are closer to real applications. Future work will focus on designing angle-based formation laws to guarantee almost global stability.

References

[1] A. Davids, "Urban search and rescue robots: From tragedy to technology," *IEEE Intell. Syst.*, vol. 17, no. 2, pp. 81–83, Mar./Apr. 2002.
[2] M. Waibel, B. Keays, and F. Augugliaro, "Drone shows: Creative potential and best practices," ETH Zurich, Zurich, Switzerland, Tech. Rep., p. 4, 2017.
[3] S.-J. Chung, U. Ahsun, and J.-J. E. Slotine, "Application of synchronization to formation flying spacecraft: Lagrangian approach," *J. Guid., Control, Dyn.*, vol. 32, no. 2, pp. 512–526, 2009.
[4] S. Zhao, "Affine formation maneuver control of multi-agent systems," *IEEE Trans. Autom. Control*, vol. 63, no. 12, pp. 4140–4155, Dec. 2018.

[5] H.-S. Ahn, *Formation Control: Approaches for Distributed Agents*, vol. 25. Berlin, Germany: Springer, 2019.
[6] B.-H. Lee and H.-S. Ahn, "Distributed formation control via global orientation estimation," *Automatica*, vol. 73, pp. 125–129, 2016.
[7] Z. Meng, B. D. Anderson, and S. Hirche, "Formation control with mismatched compasses," *Automatica*, vol. 69, pp. 232–241, 2016.
[8] H. G. de Marina, "Maneuvering and robustness issues in undirected displacement-consensus-based formation control," *IEEE Trans. Autom. Control*, vol. 66, no. 7, pp. 3370–3377, Jul. 2021.
[9] K.-K. Oh and H.-S. Ahn, "Leader-follower type distance-based formation control of a group of autonomous agents," *Int. J. Control, Autom. Syst.*, vol. 15, no. 4, pp. 1738–1745, 2017.
[10] L. Krick, M. E. Broucke, and B. A. Francis, "Stabilisation of infinitesimally rigid formations of multi-robot networks," *Int. J. Control*, vol. 82, no. 3, pp. 423–439, 2009.
[11] H. G. de Marina, B. Jayawardhana, and M. Cao, "Distributed rotational and translational maneuvering of rigid formations and their applications," *IEEE Trans. Robot.*, vol. 32, no. 3, pp. 684–697, Jun. 2016.
[12] H. G. de Marina, B. Jayawardhana, and M. Cao, "Taming mismatches in inter-agent distances for the formation-motion control of second-order agents," *IEEE Trans. Autom. Control*, vol. 63, no. 2, pp. 449–462, Apr. 2018.
[13] Z. Sun, B. D. Anderson, M. Deghat, and H.-S. Ahn, "Rigid formation control of double-integrator systems," *Int. J. Control*, vol. 90, no. 7, pp. 1403–1419, 2017.
[14] S. Zhao and D. Zelazo, "Bearing rigidity theory and its applications for control and estimation of network systems: Life beyond distance rigidity," *IEEE Control Syst. Mag.*, vol. 39, no. 2, pp. 66–83, Apr. 2019.
[15] G. Jing, G. Zhang, H. W. J. Lee, and L. Wang, "Angle-based shape determination theory of planar graphs with application to formation stabilization," *Automatica*, vol. 105, pp. 117–129, 2019.
[16] S. Zhao and D. Zelazo, "Bearing rigidity and almost global bearing-only formation stabilization," *IEEE Trans. Autom. Control*, vol. 61, no. 5, pp. 1255–1268, May 2016.
[17] M. Basiri, A. N. Bishop, and P. Jensfelt, "Distributed control of triangular formations with angle-only constraints," *Syst. Control Lett.*, vol. 59, no. 2, pp. 147–154, 2010.
[18] L. Chen, M. Cao, and C. Li, "Angle rigidity and its usage to stabilize multi-agent formations in 2D," *IEEE Trans. Autom. Control*, vol. 66, no. 8, pp. 3667–3681, Aug. 2021.
[19] L. Chen, M. Cao, H. G. de Marina, Y. Guo, and Y. Kapitanyuk, "Triangular formation maneuver using designed mismatched angles," in *Proc. 18th Eur. Control Conf.*, 2019, pp. 1544–1549.
[20] W. J. Palm, *System Dynamics*, vol. 2. New York, NY, USA: McGraw-Hill, 2010.
[21] X. Fang, X. Li, and L. Xie, "Distributed formation maneuver control of multiagent systems over directed graphs," *IEEE Trans. Cybern.*, early access, Feb. 21, 2021, doi: 10.1109/TCYB.2020.3044581.
[22] Q. Van Tran and H.-S. Ahn, "Distributed formation control of mobile agents via global orientation estimation," *IEEE Trans. Control Netw. Syst.*, vol. 7, no. 4, pp. 1654–1664, Dec. 2020.
[23] T.-S. Tay and W. Whiteley, "Generating isostatic frameworks," *Struct. Topology*, no. 11, pp. 21–69, 1985.
[24] I. Buckley and M. Egerstedt, "Infinitesimal shape-similarity for characterization and control of bearing-only multirobot formations," *IEEE Trans. Robot.*, vol. 37, no. 6, pp. 1921–1935, Dec. 2021.
[25] R. A. Horn and C. R. Johnson, *Matrix Analysis*. Cambridge, U.K.: Cambridge Univ. Press, 2012.
[26] M. Marden, *Geometry of Polynomials*. Providence, RI, USA: Amer. Math. Soc., 1949.
[27] L. Chen, H. G. de Marina, and M. Cao, "Maneuvering formations of mobile agents using designed mismatched angles," *IEEE Trans. Autom. Control*, early access, Mar. 17, 2021, doi: 10.1109/TAC.2021.3066388.

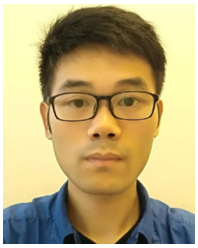

Liangming Chen (Member, IEEE) received the B.E. degree in automation from Southwest Jiaotong University, Chengdu, China, in 2015. From 2015 to 2021, he enrolled jointly in the Ph.D. programs of systems and control in the Harbin Institute of Technology, Harbin, China, and the University of Groningen, Groningen, The Netherlands.

His current research interests include rigidity theory, formation control, and multiagent systems.

Mingming Shi received the B.Eng. degree in spacecraft design and engineering, the M.Eng. degree in aeronautical and astronautical science and technology from the Harbin Institute of Technology, Harbin, China, in 2013 and 2015, respectively, and the Ph.D. degree in control theory from the Faculty of Science and Engineering, University of Groningen, Groningen, The Netherlands, in 2019.

He is currently a Postdoctoral Researcher with the Université Catholique de Louvain, Ottignies-Louvain-la-Neuve, Belgium. His research interests include networked control systems and sensor networks.

Hector Garcia de Marina received the M.Sc. degree in electronics engineering from the Complutense University of Madrid, Madrid, Spain, in 2008, the M.Sc. degree in control engineering from the University of Alcala, Alcala de Henares, Spain, in 2011, and the Ph.D. degree in systems and control from the University of Groningen, Groningen, The Netherlands, in 2016.

He held a Postdoctoral position with the Ecole Nationale de l'Aviation Civile', Toulouse, France, from 2016 to 2018. From 2018 to 2020, he was an Assistant Professor with the Unmanned Aerial Systems Center, University of Southern Denmark, Odense, Denmark. In 2020, he was a Research Fellow with the Complutense University of Madrid. Currently, he is a Research Fellow with the University of Granada, Granada, Spain, under the Ramon y Cajal program. His research interests include the guidance navigation and control for autonomous robots, and multiagent systems.

Dr. de Marina is an Associate Editor for the IEEE TRANSACTIONS ON ROBOTICS.

Ming Cao (Fellow, IEEE) received the bachelor's and master's degrees from Tsinghua University, Beijing, China, in 1999 and 2002, respectively, and the Ph.D. degree from Yale University, New Haven, CT, USA, in 2007, all in electrical engineering.

He is currently a Professor of Systems and Control with the Engineering and Technology Institute (ENTEG), University of Groningen, Groningen, The Netherlands, where he started as an Assistant Professor in 2008. From 2007 to 2008, he was a Postdoctoral Research Associate with the Department of Mechanical and Aerospace Engineering, Princeton University, Princeton, NJ, USA. He worked as a Research Intern in 2006 with the Mathematical Sciences Department, IBM T. J. Watson Research Center, Ossining, NY, USA. His main research interests include autonomous agents and multiagent systems, decision-making dynamics, and complex networks.

Dr. Cao was the inaugural recipient of the Manfred Thoma medal in 2017 from the International Federation of Automatic Control (IFAC) and the recipient of the European Control Award sponsored by the European Control Association (EUCA) in 2016. He is a Senior Editor for *Systems and Control Letters*, an Associate Editor for IEEE TRANSACTIONS ON AUTOMATIC CONTROL, IEEE TRANSACTIONS ON CIRCUITS AND SYSTEMS, and *IEEE Circuits and Systems Magazine*.